Experimental and CFD Analysis of a Gas-Lubricated Foil Thrust Bearing for Various Foil Configurations

Ravikumar R N
Associate Professor
Department of Mechanical Engineering
BMS College of Engineering
Bangalore-560019
India

Rathanraj K J
Professor
Department of Industrial Engineering and Management, BMS College of Engineering
Bangalore-560019
India

Arun Kumar V
Adjunct Professor
Department of Mechanical Engineering
BMS College of Engineering
Bangalore-560019
India

Supreeth S
PhD Research Scholar
Department of Mechanical Engineering
Dr. Ambedkar Institute of Technology
Bangalore-560056
India

Thrust foil bearings operating at hydrodynamic conditions are self-acting (aerodynamic) bearings that support high-speed shafts at mild loading conditions with air as a lubricant and are generally used in low-power gas turbines. This paper presents an experimental study and a detailed computational analysis of dynamic characteristics of the foil thrust bearing (FTB) in terms of load-carrying capabilities as a function of thrust runner speed and gap between the bearing assembly and the runner by considering the effect of bearing parameters such as number of foils, shape of the foils, and assembly of foils on the bearing pad. The parametric study was conducted on a newly conceptualized bearing test rig capable of rotating up to 45,000 rpm speeds that measured the axial loads of the air foil thrust bearings (AFTB). The computational model of the foil thrust bearings for various configurations with top foils is simulated using multiphysics software for foil deflections and pressure distributions on the foil surface. The numerical results were compared with the experimental values, while the air foil thrust bearings with multilayered foils called cascaded foils (patented) had higher load capability in comparison to other conventional bearing models.

Keywords: *Self-acting, air foil thrust bearing, cascaded foils, square foils, wedge film, pressure profile, and stiffness.*

1. INTRODUCTION

Foil bearings are self-acting hydrodynamic bearings supporting lightly loaded high-speed shafts with physically non-contact operation using fluid (typically air) as a medium in hostile environments. The gas or air that is present in between the high-speed runner and the foil acts as a lubricating medium and supports the axial load at high speed due to the formation of air wedge film, while the foil provides damping and stiffness. Basically, air foil thrust bearing (AFTB) operates under two conditions: one is hydrodynamic, and the other is by hydrostatic condition. In the hydrodynamic mode of operation, the bearing is termed as self-acfting, and the load is supported only due to the formation of an air wedge film between the foil assembly and the runner by which the air pressure increases. Whereas in the case of hydrostatic bearing, pressurized air is supplied externally through an orifice between the runner and foil assembly that carries the load acting on the bearing at low-speed operation. In order to accomplish the required load-carrying capabilities, accurate manufacturing with improved foil design of air-lubricated foil bearings is necessary for their effective operation at higher speeds. The benefits of these bearings in high-speed turbo machinery are significant and include reduced weight, reliability, contamination-free environment, high-temperature operation, and absolute use of lubricant [1]. Some major limitations of these bearings are namely lower capacity than roller or oil bearings, wear during start-up and stop cycles, and require high speed for operation. The most common applications of these thrust foil bearings include high-speed turbines, food processing industries, aircraft, aircraft cooling turbines, lightly loaded gas turbine engines, and air cycle machines.

Earlier theoretical models and numerical studies on foil thrust bearings (FTB) by H Heshmat and others [2] on converging foil geometry are phenomenal in obtaining fluid film thickness and foil pressure profiles. Numerical plots on pressure distribution and foil deflection of hybrid air foil thrust bearings (HAFTB) for various design and operating parameters by Lee and Kim [3], FEA modeling and simulation in COMSOS by C A Heshmat et al. [4], pressure profiles for various film thickness ratios of FTB by Gad and Kaneko [5], fluid film thickness and pressure contours of gas foil thrust bearing (GFTB) for lower speeds obtained by Kim et al. [6], and gas film thickness with surface pressure on novel GFTB with taper grooves by Hu and Feng [7] were beneficial in providing boundary conditions for the present work. Fluid-thermal-structure-interaction studied by Cheng Xiong and others [8] for an AFTB of 47 mm diameter at 151krpm speeds, analysis of annular top foil by Markus et al. [9] for an AFTB of 54 mm diameter up to 120krpm speeds, and numerical analysis with rectangular grooves on the top foil for an AFTB of 38 mm diameter at 30,000 rpm speeds played a significant role in modeling and simulation of the present work. Theoretical and

Received: July 2023, Accepted: September 2023
Correspondence to: Mr. Supreeth S, PhD Research Scholar, Department of Mechanical Engineering, Dr. Ambedkar Institute of Technology, Bangalore-560056, India. E-mail: supreeth.s1994@gmail.com
doi: 10.5937/fme2304532R

numerical investigations by Wu and Hu [10] analyzed the change in lubrication of an AFTB during start and stop cycles by concluding that an increase in surface roughness increases the lift-off speed and, hence, the contact time. Multiphysics CAE simulation by Yu and Wang [11] verified the accuracy of the computational method by building a 3D fluid-structure interaction (FSI) model of GFTB manifested pressure and temperature distribution along with foil displacements. Experimentations by Supreeth S et al. [12, 13] on foil thrust bearings with various top foil configurations at different speeds, along with simulations in ANSYS, threw awareness on the term foil stiffness. Some experimentations by R N Ravikumar and others [14, 15] on top foil configurations added enormous knowledge to the present study. Few review literature [16-18] furnished deeper knowledge on numerous research gaps and factors affecting the load capabilities of FTB.

Oil-film pressure on the journal bearing lubricated with various lubricants was analyzed by Ramaganesh R et al. [19], and Diaphragm deformation of a piezo-resistive pressure microsensor was analyzed by F. Pashmforoush [20] using COMSOL multiphysics helped in pressure boundary conditions for the present AFTB modeling and simulations. From the literature survey, it is evident that the performance of foil bearings is mainly defined in terms of load-carrying capabilities and is often considered a better choice with respect to conventional oil bearings due to their use in relatively high-speed applications. The current study comprises testing AFTB with four copper foil arrangements (without bump foil) on a bearing test rig that is developed for the purpose along with CFD simulation for validation and hence selects the optimum foil design that enhances the load-carrying capability. Various literature on AFTB by numerous scientists and researchers have considered the top foil with bump foil and or viscoelastic supports for their analysis, while no literature is available on foil thrust bearing without bump foil. This paper mainly focuses on gas foil bearing without bump foil, which reduces the design's complexity and increases the top foil stiffness along with newly conceptualized cascaded foils (patented).

2. EXPERIMENTATION

The bearing test rig is an instrumented equipment that measures the axial load, operating speed, and the dis–tance between the bearing (foil tip) and the thrust runner.

The AFTB test rig is pictured in Fig. 1, and the foil thrust bearing assembly is in Fig. 2. The thrust runner made of aluminum alloy (60 mm diameter with 10 mm thickness) mounted on a turbocharger that is driven by an air compressor is capable of operating up to 45,000 rpm speeds.

The thrust foil bearing assembly is placed parallel to the runner vertically (Fig. 2) and is mounted beneath the S-shaped load cell that measures the axial load (N) on the bearing having to and fro displacement (mm). The magnetic probe measures the thrust runner's operating speed (rpm), which carries two neodymium magnets on either side (embedded in the circumference of the thrust runner). Copper sheets are used as foils in the present study that are prepared using wire electrical discharge machining (EDM) and bent using a machine vice. These foils are fixed on the bearing pad made up of 3D printing technology (silver metallic) with 60 mm diameter and 12 mm thickness.

The two main foil shapes depicting the inner edge (IE) and outer edge (OE) are sketched in Fig. 3, and it is observed that the height of the IE and the OE of the angular foils of FTB plays a significant role in load bearing capability. Throughout the paper, IE≠OE represents the height of IE and OE are different, i.e., the leading edge (free end) of the foil is not parallel to the runner or to the bearing pad surface. Similarly, IE=OE represents the height of IE and OE the same, i.e., the foil's leading edge is parallel to the runner or to the bearing pad surface. It is found that the air wedge over the foil varies both radially and circumferentially for FTB with foils having IE≠OE, while the air wedge over the top foil has a constant radial width and varies circumferentially for FTB with foils having IE=OE. The parameters of the GFTB considered for the present study are given in Table 1.

The experimentation includes measuring thrust loads of the air foil bearing with four different foil confi–gurations as below:

1. AFTB with square-shaped foils
2. AFTB with angular foils (IE≠OE)
3. AFTB with angular foils (IE=OE)
4. AFTB with cascaded foils (IE=OE)

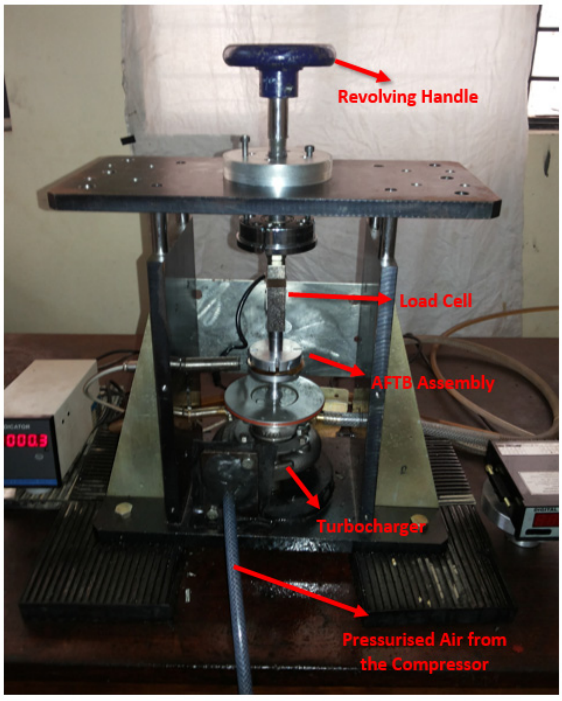

Figure 1. AFTB test rig

The dimensions of the square foil are 22 mm by 22 mm with a thickness of 0.2 mm and an inclination of 12.8°. The dimensions of the angular foils (for both cases) are about 8 mm inner radius and 30 mm outer radius with a thickness of 0.2 mm. The geometry of the angular foil with IE=OE is slightly modified by inc–reasing the length of the trailing edge of the fixing edge of the foil by 4.5 mm. Cascaded foils or multilayered foils (Indian Patent granted with reference no. 3663 /CHE/2015 and patent no. 420041) are prepared by

fixing the angular foils of different sector angles on the bearing pad such as the foil of largest sector angle is placed at the bottom and the rest of the foils placed over it in descending order of sector angles. In the present study, three foils in cascaded configuration with sector angles of 90°, 67°, and 48° for bottom, intermediate, and top foil, respectively, are considered, while the thickness of the bottom foil being 0.2 mm and that of the other two foils having 0.1 mm each.

Throughout the study, GFTB with three foils of each configuration on the bearing pad are tested. The post-tested bearing assembly with wear and tear of foils is depicted in Fig. 4.

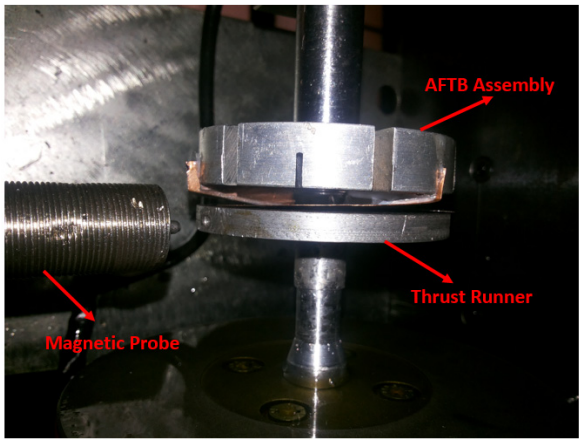

Figure 2. Thrust foil bearing assembly

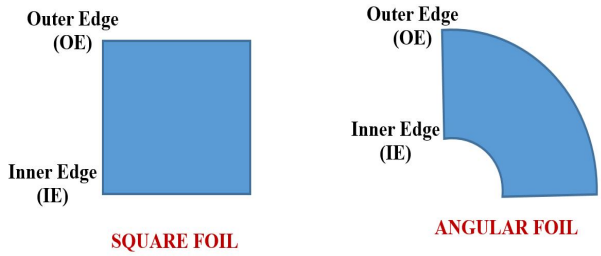

Table 1. Specifications of the proposed AFTB

The inner radius of the foil, r_1	8 mm
The outer radius of the foil, r_2	30 mm
Foil material	EC Copper
The sector angle of the foil, β	90º
Foil Inclination Angle, α	12.8º
Top foil thickness considered	0.2mm
Operating speeds considered	10 krpm, 15 krpm, 20 krpm, 25 krpm, 30 krpm, 35 krpm, 40 krpm, and 45 krpm.

Figure 3. Two main foil shapes

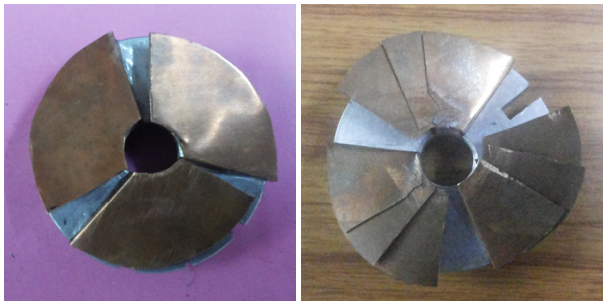

(a) (b)

Figure 4. Post-tested AFTB with (a) angular foils (IE=OE) and (b) cascaded foils (IE=OE)

3. SIMULATION

Modeling and analysis of a gas foil thrust bearing are mostly limited to simple cases with rigid geometry and constant lubricant properties, although they require ex–pensive software and computing configurations. Analy–tical modeling has advanced with increased computing power such that advanced numerical modeling can be conducted relatively cheaply and quickly. Computa–tional analysis has been carried out to ensure the pressure developed on various types of thrust foil bearings at different speeds in the present study. Based on the pressure developed on the foil surface, the load-carrying capacity of the FTB is determined while the foil deflections and stresses are also noted. The present computational fluid dynamics (CFD) of FTB obtained in COMSOL multiphysics software (being a pre-processor, a solver, and a post-processing phase) uses the concept of finite element analysis to solve real-time problems. Compared to other software, COMSOL has a physics-based interface, which allows users to define the required partial differential equations. All four foil configurations of GFTB are modeled using the NX CAD software, as pictured in Figure 5, before importing for simulation.

COMSOL multiphysics is used to analyze different foil arrangements of air foil thrust bearing to simulate pressure distribution, stress, and displacement of the foil. A general overview of the procedure developed to analyze the AFTB is explained in detail.

➢ **Variables and Materials**

The variables used in the present analysis are presented in Table 2. The fluid boundary (rectangular sector) is assigned with air as a material with 1 kg/m^3 as the density and 1.983e-5 Pa*sec as the dynamic viscosity. The foil (structural domain) is assigned with copper as the material, with 8954 kg/m^3 as the density, 0.33 as the poison's ratio, and 110e^9 Pa as Young's modulus.

➢ **Boundary Conditions**

Free deformation boundary conditions are provided to the fluid domain, and all the surfaces of the rectangular sector except the rectangular faces are selected as walls, which defines the fluid flow path. The fluid domain is selected and assigned with a prescribed mesh boundary displacement condition that defines the deformation of the fluid mesh corresponding to the deformations of the foil and the rotation of the runner.

➢ **Fluid-Structure Interaction (FSI)**

The foil is selected and given FSI boundary condition (as shown in figure 6 (a) for cascaded foils). Since the assumed foil material (copper) is linearly elastic, the entire foil is selected as a linear elastic material that defines the linear stress-strain variation in the material.

➢ **Open Boundary**

The open boundary node is used to set up mass transport across boundaries where both inflow and outflow can occur. This outflow condition applies to the parts of the boundary where fluid flows in and out of the domain. The side walls of the fluid domain are selected as open boundaries, as shown in Figure 6 (b).

➢ **Moving Wall**

The top surface of the fluid domain is selected as a moving wall boundary condition (as in Figure 6 (c)).

Previously defined and derived variables u, v, and w are specified in the velocity field corresponding to the x, y, and z direction for the moving wall, which in turn specifies the rotary motion of the runner.

➢ **Constraints**

The key, which is in contact with the foil and the bottom surface of the fluid domain, is selected as a fixed constraint (i.e., displacement at all directions is zero), which idealizes the foil as an inclined cantilever beam. The selected fixed constraint of the foil is shown in Figure 6 (d).

➢ **Meshing**

The size of the mesh to be created for the model is specified as a course, which is calibrated to fluid dynamics mode in COMSOL. The element type of the mesh is defined as free tetrahedral, and the meshing is performed over the entire geometry, while the software considers finer mesh elements at complex sections (Figure 6(e)).

➢ **Solving**

This problem is solved under steady state dynamic con–ditions with displacement of the runner in the Z-direc–tion being assumed as zero. There is no contact between the top foil and the runner surface at start and stop cyc–les as in the experimental case, while the same is assu–med (or provided) with some clearance (in microns).

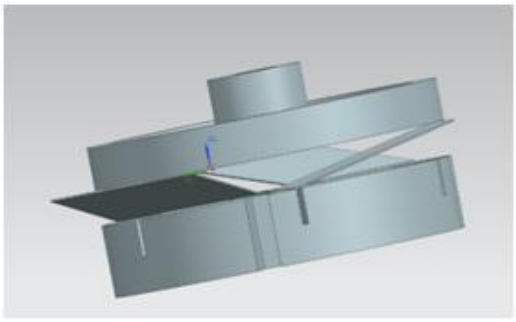

(a)

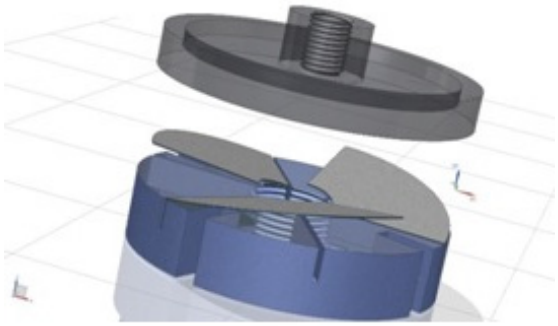

(b)

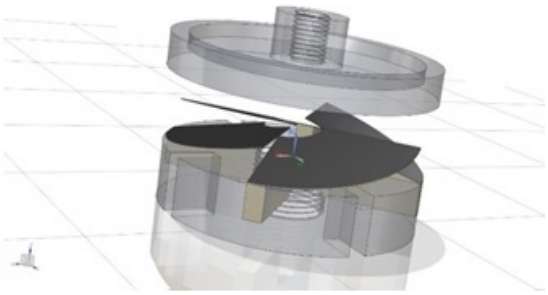

(c)

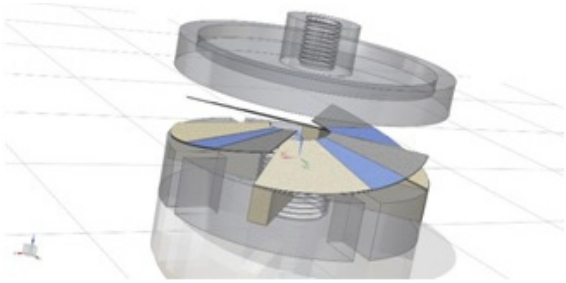

(d)

Figure 5. AFTB model with (a) square foils, (b) angular foils having IE ≠ OE, (c) angular foils having IE = OE, and (d) cascaded foils

Table 2. Variables of CFD study

Name	Expression	Description
r	sqrt(z ^ 2 + y ^ 2)	radial coordinate zy-plane
omega	2*pi*30000/60[rad/s]	angular velocity
phi	atan2(z, y)	azimuthal angle
u	0[m/s]	rotor velocity in x-direction
v	omega*r*sin(phi)	rotor velocity in y-direction
w	-omega*r*cos(phi)	rotor velocity in z-direction

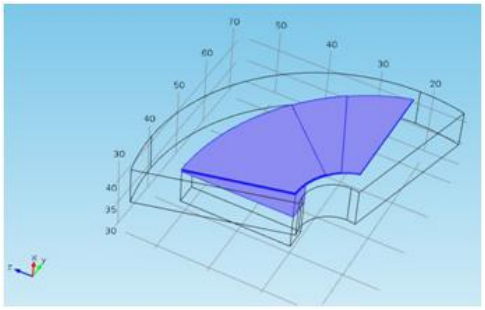

(a)

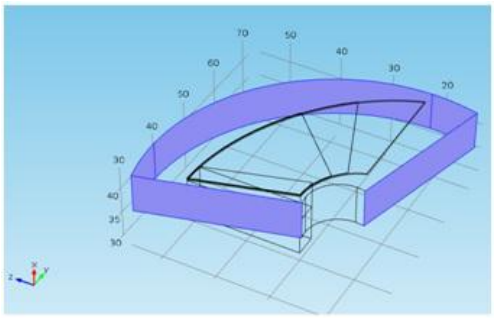

(b)

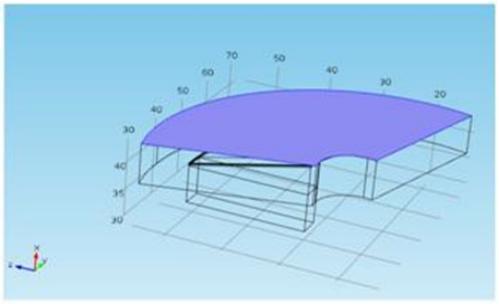

(c)

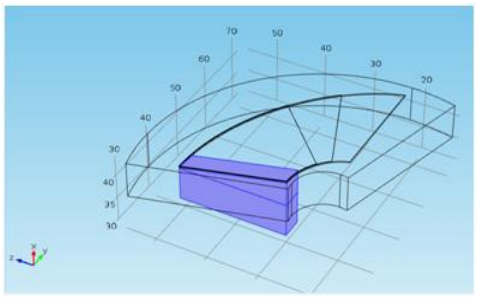

(d)

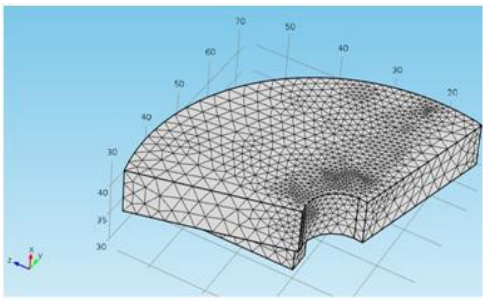

(e)

Figure 6. (a) Fluid-structure interaction (FSI) boundary for cascaded foils, (b) open boundary walls, (c) moving wall of the fluid domain, (d) fixed constraint of the foil structure, and (e) meshing

4. RESULTS AND DISCUSSIONS

Experimentations were conducted for all FTBs with four different foil arrangements for dynamic conditions in terms of load-bearing capability for operating speeds catering up to 45,000 rpm. Three square foils are fixed on the bearing pad and are mounted parallel to the thrust runner, with the minimum distance between the runner and the foil being zero. Once the runner is operated at 10,000 rpm, the thrust load is noted from the load indicator and similarly for all other possible speeds of the test rig. This procedure is repeated for three angular foils (IE≠OE and IE=OE) and cascaded foils with all the values being plotted in Figure 7(a). From the graph, it is evident that the axial load of an AFTB is directly proportional to operating speeds, while the cascaded foil AFTB carries the highest loads in comparison to other foil combinations. Angular foils with IE≠OE have the least load-carrying capacity because only a small portion of foil resists air flow, and hence the pressure developed is small. It is observed that the square foil configuration has a larger load-bearing capacity as the larger portion (surface) of the foil resists the fluid flow, leading to larger pressure developed with a greater radial length. Hence, the foil material is utilized to its full capacity, unlike in the IE≠OE case, wherein there is not much improvement in the load-bearing capabilities. Moreover, the angular foil with the configuration of IE=OE has a higher load-carrying capacity (greater pressure) than that of square foils because of the larger circumferential surface that resists the air flow.

It can also be seen that the load reaches higher at 40,000 rpm, and then it decreases due to increased deflection at increased speed, resulting in increased film thickness. This speed versus load graph depicts that at higher speeds, the load capacity of the foil increases nevertheless for a tolerable range of speed. In cascaded configured foil thrust bearing (patented), the highest load capacity is observed due to an increase in number of foils that increases the foil stiffness of the bearing. This trend is observed at different speeds throughout the study. As the number of foils increases, the formation of uniform wedge film increases in the radial direction, which enhances the load-carrying capabilities of the AFTB and, hence, the optimized foil configuration. FTB with single foil, two foils, and three foils for all foil configurations are mounted on the bearing pad and tested for 45,000 rpm speeds, as plotted in Figure 7(b). This eventually concludes that load bearing capability of an AFTB increases linearly with an increase in the number of foils for any type of foil configuration.

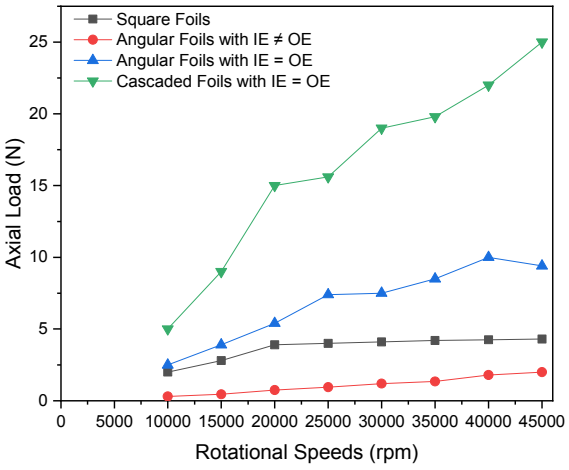

(a)

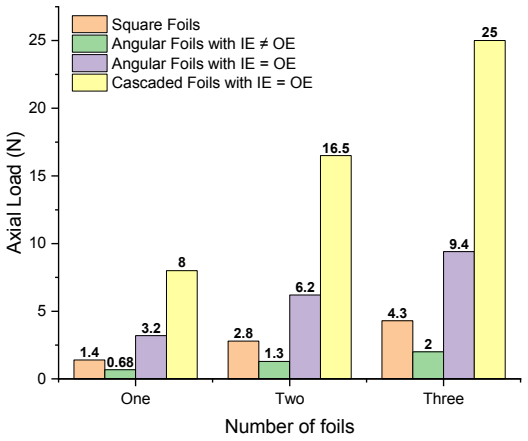

(b)

Figure 7. (a) Load capacity of the FTB for all foil configu–rations (b) Load capacity of AFTB with varying numbers of foils at 45,000 rpm

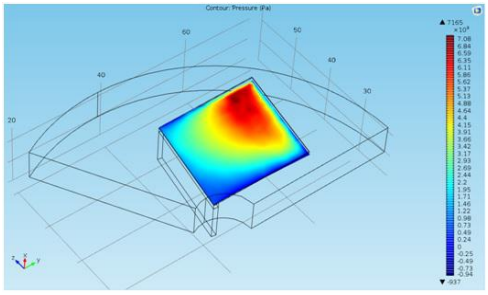

(a)

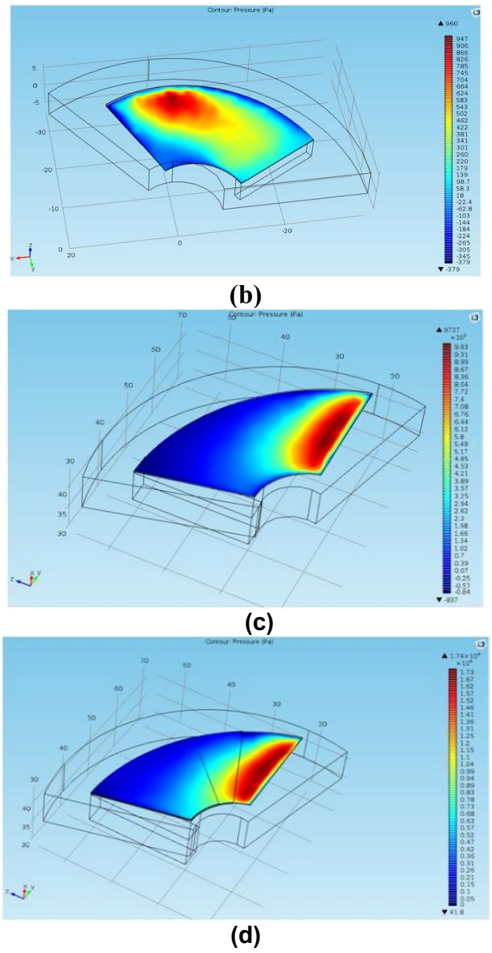

Figure 8. Pressure distribution plots for (a) square foil, (b) angular foil with IE≠OE, (c) angular foil with IE=OE, and (d) cascaded foil

The importance of the CFD study is to analyze the pressure profile and deflection of the foil of an air foil thrust bearing for all the mentioned foil arrangements. Figure 8 shows the pressure distribution obtained after steady state dynamic analysis of the modeled AFTB for different configurations of foils with 0.2 mm top foil thickness at 30,000 rpm. In this study, the operation speeds of the bearing test rig that is limited up to 45,000 rpm, whereas in CFD simulations, the rotational speeds can be given higher. The major assumptions of the simulation study are the course meshing, the fluid boundary being limited up to the bearing assembly, and steady-state dynamic analysis. These assumptions are majorly made in reducing the computational solving time. The simulations are solved for all operating speeds from 10,000 rpm to 45,000 rpm, and in all cases, the pressure is high at the tip of the top foil (almost near to the free end of the foil) where the air film thickness is minimum. These results are in agreement with the theoretical predictions of the various AFTB mathe–matical models developed by previous researchers and scientists.

As the initial contact between the thrust runner (moving wall) and the top foil is more in the case of IE=OE, there is more pressure developed in this case as compared to that of IE≠OE from the plots. Since the foil leading edge undergoes some deflection, the maximum pressure point gets shifted circumferentially inwards. Although the pressure distribution in the case of cascaded and angular foils with IE=OE appears to be similar, at high speeds, the maximum pressure region shifts radially inward in the case of IE=OE, which is lesser in comparison to cascaded or multilayered foils. Similarly, the deflection of foils is analyzed for all configurations of foil assembly. From the contour plots shown in Figure 9, it is observed that the deflection is more at the tip of the foil.

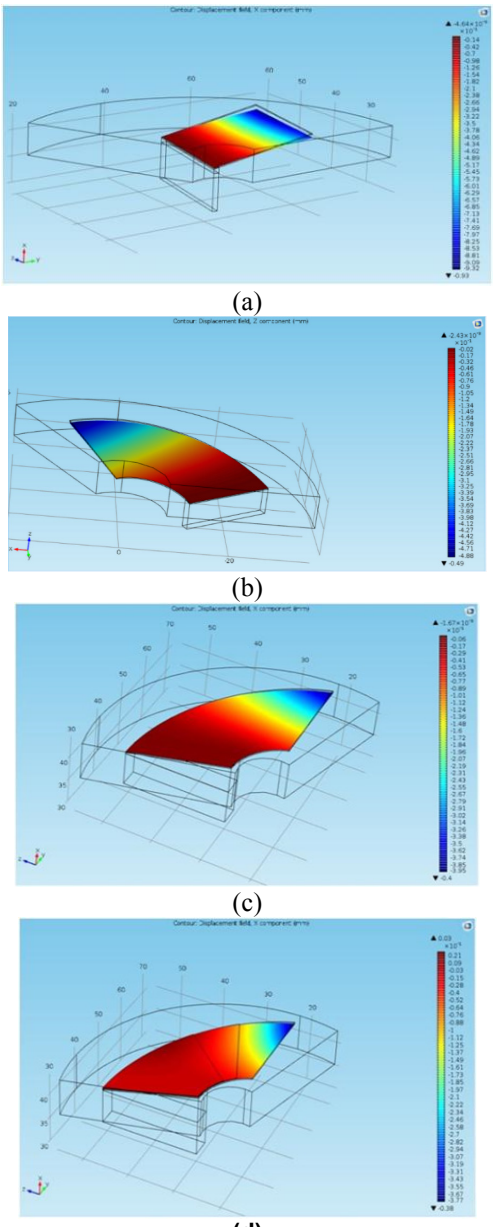

Figure 9. Deflection contour plot of (a) square foil, (b) angular foil with IE≠OE, (c) angular foil with IE=OE, and (d) cascaded foil

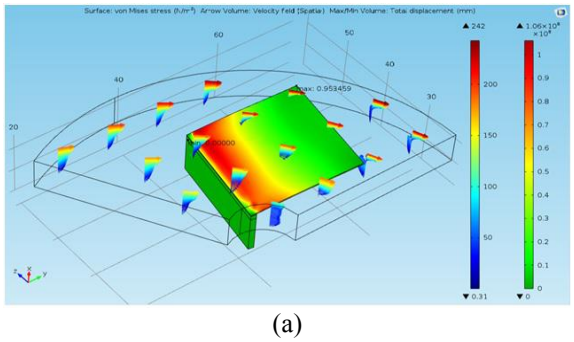

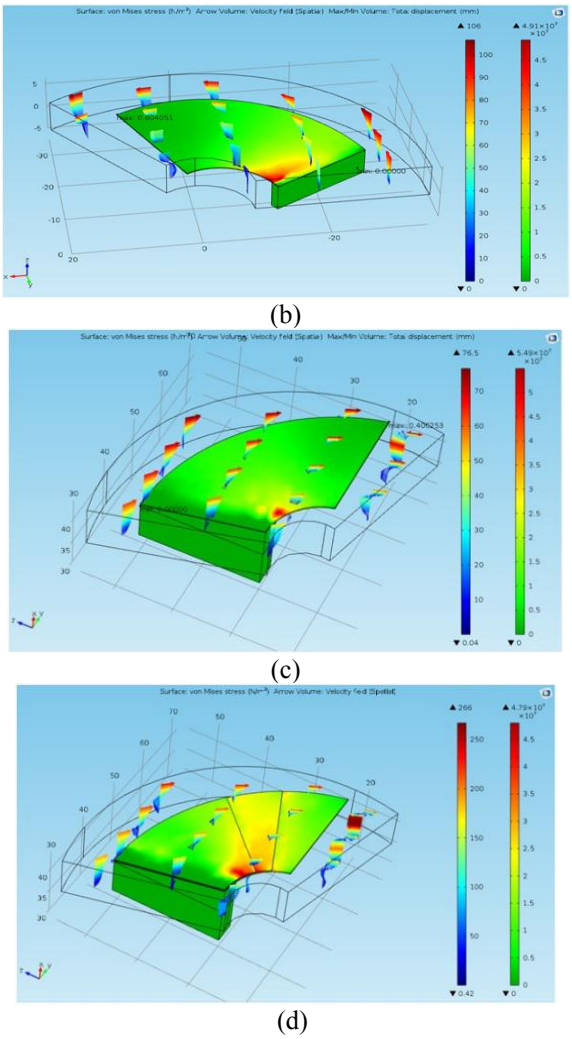

Figure 10. Stress contour plot for (a) square foil, (b) angular foil (IE≠OE), (c) angular foil (IE=OE), and (d) cascaded foil

The foil inherits the behavior of an inclined cantilever beam, and the order of deflection is higher at higher rotational speeds. Also, it is observed that the surface stress distribution is fairly even throughout the foil-bearing configurations, mainly because the fluid load is almost constant during dynamic analysis. Figure 10 shows that the maximum stress is at the fixed end of the foil, as the foil assembly resembles a cantilever beam.

A parametric sweep study was conducted at different running speeds of the AFTB under the same operating boundary conditions and foil dimensions. The deflection and pressure distribution results obtained for the simu–lated air foil thrust bearings at runner speeds ranging from 10,000 rpm to 45,000 rpm are noted. The pressure distribution in terms of axial (thrust) loads for all speeds is charted in Figure 11(a), while the foil deflection for all speeds is charted in Figure 11(b). It can be observed from these graphs that as the foil deflections are higher, the load-carrying capability increases for all foil configurations. The comparisons between experimental values and COMSOL data for load-carrying capabilities for different foil configurations are shown in Figures 12 and 13. The experimental values almost agree with the computational results, and the cascaded (multilayered) foil configuration AFTB has a higher load-carrying capability than all other configurations.

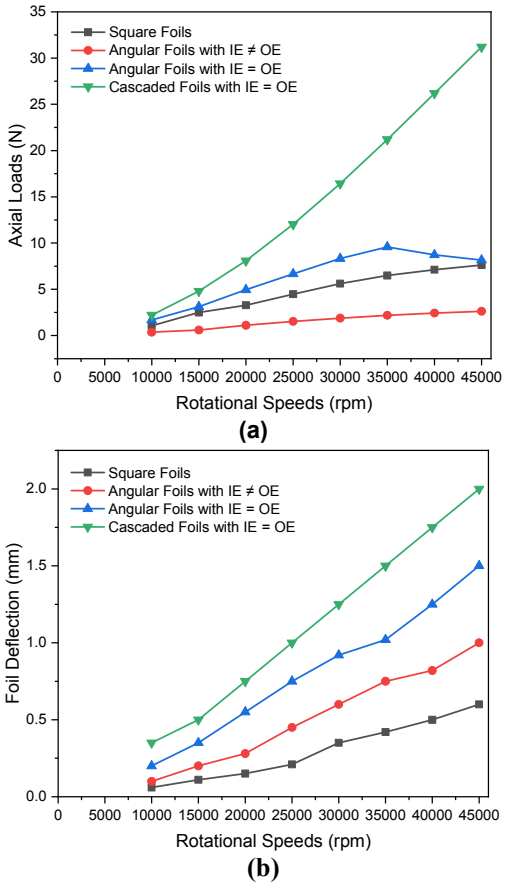

Figure 11. (a) Load capacity and (b) foil deflection plots for different foil arrangements of AFTB

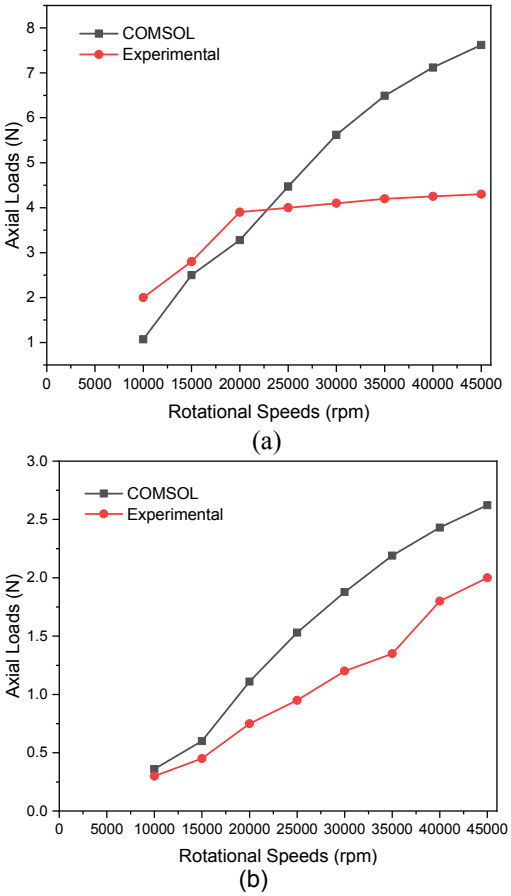

Figure 12. Comparison of load capacity between experimental and COMSOL results for (a) square foils and (b) sector or angular foils with IE≠OE

5. CONCLUSIONS

The present study on AFTB with four different foil configurations operating up to 45,000 rpm evaluates the bearing's performance in terms of load capacity. The dynamic characteristics of FTB are dependent on various parameters, such as the gap between the foil and runner, the shape of the foils, the speed of the runner, and the effect of cascading. From the experimental research work, it could be seen clearly that a simple foil thrust bearing of 60 mm diameter is able to support a substantial amount of thrust load, which can be compared to the existing air foil thrust bearing where bump foils are used with the top foil.

Computational analysis in COMSOL multiphysics configured the pressure distribution, foil deflection, and stress contours for AFTB with square foils, angular foils with IE≠OE and IE=OE, and cascaded foils with IE= OE. Angular foil with IE≠OE had the least load-carrying capacity compared to square foil due to a small portion of the foil surface resisting the gas flow. Whereas the angular foil with the configuration of IE=OE has enhanced load carrying capacity than square foils, cascaded foils with three angular foils with IE=OE supported larger loads due to the number of wedge films.

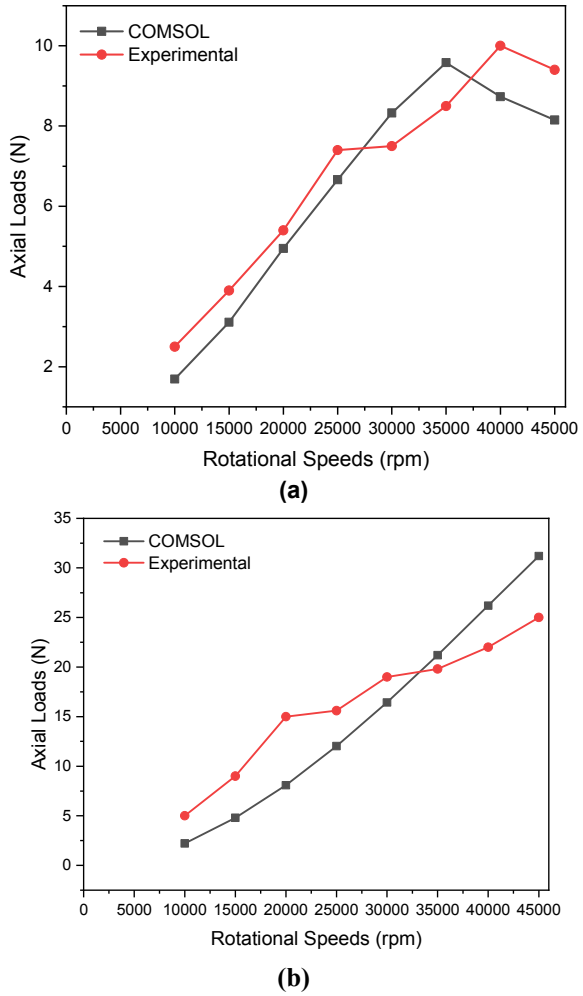

Figure 13. Comparison of load capacity between experimental and COMSOL results for (a) sector foils with IE=OE and (b) cascaded sector foils with IE=OE

The variation of foil deflection for all four foil configurations for different speeds indicates that as the foil deflection is lesser, the load-carrying capability is higher. The experimental and CFD data of all AFTB foil arrangements are in concurrence, while the multilayered foils carried higher thrust loads.

ACKNOWLEDGMENTS

The authors owe their gratitude towards AICTE for funding the present research study towards developing a novel bearing test rig, patent application charges, and other consumables. Also, the authors acknowledge the Department of Mechanical Engineering, BMS College of Engineering, Bangalore, towards the computer simulations.

DECLARATION OF CONFLICTING INTERESTS

The authors declare that they have no potential conflicts of interest with respect to the research, authorship and or publication of this article.

REFERENCES

[1] Giri L. Agarwal, "Foil air/gas bearing technology - An overview," Proc. ASME Turbo Expo, vol. 345E, 1997, doi: 10.1115/97-GT-347.

[2] J. A. W. Heshmat. H, O. Pinkus, "Analysis of Gas Lubricated Compliant Thrust Bearings," Trans. ASME, vol. 105, pp. 638–646, October 1983.

[3] D. Lee and D. Kim, "Design and performance prediction of hybrid air foil thrust bearings," J. Eng. Gas Turbines Power, vol. 133, no. 4, pp. 1-13, 2011, doi:10.1115/1.4002249.

[4] C. A. Heshmat, D. S. Xu, and H. Heshmat, "Analysis of gas lubricated foil thrust bearings using coupled finite element and finite difference methods," Journal of Tribology, vol. 122, no. 1, pp. 199–204, 2000, doi:10.1115/1.555343.

[5] A. M. Gad and S. Kaneko, "A new structural stiffness model for bump-type foil bearings: Application to generation II gas lubricated foil thrust bearing," Journal of Tribology, vol. 136, no. 4, 2014, doi:10.1115/1.4027601.

[6] T.H. Kim et al. "Design Optimization of Gas Foil Thrust Bearings for Maximum," J. Tribol., vol. 139, pp. 1–11, 2017, doi:10.1115/1.4034616.

[7] H. Hu and M. Feng, "Performance of novel air foil thrust bearings with taper-groove on surface of top foil," Proc. Inst. Mech. Eng. Part J J. Eng. Tribology, vol. 235, no. 1, pp. 79–92, 2021, doi:10.1177/1350650120925338.

[8] C. Xiong, B. Xu, H. Yu, Z. Huang, and Z. Chen, "A thermo-elastic-hydrodynamic model for air foil thrust bearings considering thermal seizure and failure analyses," Tribology International, vol. 183, February 2023, doi:10.1016/j.triboint.2023.108373.

[9] M. Eickhoff, A. Theile, M. Mayer, B. Schweizer, "Analysis of Air Foil Thrust Bearings with annular top foil including wear prediction, Part I: Modeling and simulation," Tribology International, vol. 181, June 2022, 2023, doi:10.1016/j.triboint.2022.108 174.

[10] F. Wu and Y. Hu, “Theoretical Investigations on Tribological Properties of Air Foil Thrust Bearings during Start-Up Process,” Lubricants, vol. 11, no. 3, p. 94, 2023, doi:10.3390/lubricants11030094.

[11] T. Y. Yu and P. J. Wang, "Simulation and Expe–rimental Verification of Dynamic Characteristics on Gas Foil Thrust Bearings Based on Multiphysics Three-Dimensional Computer Aided Engineering Methods," Lubricants, vol. 10, no. 9, 2022, doi:10.3390/lubricants10090222.

[12] S. Supreeth, R. N. Ravikumar, T. N. Raju, and K. Dharshan, “Foil stiffness optimization of a gas lubricated thrust foil bearing in enhancing load carrying capability,” Materials Today: Proceedings, vol. 52, pp. 1479-1487, 2022, doi:10.1016/j.matpr .2021.11.210.

[13] S. Supreeth, et al. “Parametric Studies on Performance of Oil-Free Thrust Foil Bearings at Lower Speeds,” Tribol. Ind., vol. 45, no. 1, pp. 81–88, 2023, doi: 10.24874/ti.1407.11.22.12.

[14] R. N. Ravikumar, K. J. Rathanraj, V. Arunkumar, “Comparative Experimental Analysis of Load Carrying Capability of Air Foil Thrust Bearing for Different Configuration of Foil Assembly,” Procedia Technology, vol. 25, pp. 1096-1105, September 2016, doi:10.1016/j.protcy.2016.08.215.

[15] R. N. Ravikumar, K. J. Rathanraj, V. Arunkumar, “Experimental Studies on Air Foil Thrust Bearing Load Capabilities Considering the Effect of Foil Configuration,” Appl. Mech. Mater., vol. 813–814, pp. 1007–1011, 2015, doi: 10.4028/www.scientific .net/amm.813-814.1007.

[16] R. J. Bruckner, “Performance of Simple Gas Foil Thrust Bearings in Air,” Supercrit. CO2 Power Cycle Symp., no. February, 2011.

[17] S. Shivakumar, T. Nagaraju, R. N. Ravikumar, M. C. Rudraiah, "A Review on Performance Charac–teristics of an Air Foil Thrust Bearing," Tribol. Online, vol. 17, no. 4, pp. 276–282, 2022, doi: 10.2474/trol.17.276.

[18] Rathanraj, K.J., Ravikumar R.N., “Review A Research trends in Air foil thrust bearings used in micro turbines and aircraft machines,” Int. J. Emerg. trends Eng. Dev., vol. 2, pp. 13–24, October 2016.

[19] Ramaganesh R, et al. “Finite element analysis of a journal bearing lubricated with nano lubricants”, FME Transactions, vol 48, issue 2, pp. 476-481, 2020, doi:10.5937/fme2002476R.

[20] F. Pashmforoush, "Multiphysics Simulation of Piezo-resistive Pressure Microsensor Using Finite Element Method", FME Transactions, vol 49, issue 1, pp. 214-219, 2020, doi:10.5937/fme2101214P.

ABBREVIATIONS

AFTB	Air Foil Thrust Bearings
FTB	Foil Thrust Bearings
GFTB	Gas Foil Thrust Bearings
HAFTB	Hybrid Air Foil Thrust Bearings
CFD	Computational Fluid Dynamics
EDM	Electrical Discharge Machining
IE	Inner Edge of the foil
OE	Outer Edge of the foil
IE≠OE	Inner Edge unequal to Outer Edge of the Foil
IE=OE	Inner Edge equal to Outer Edge of the Foil
3D	Three Dimensional model
FSI	Fluid- Structure Interaction
EC	Electrolytic Copper
RPM	revolutions per minute

ЕКСПЕРИМЕНТАЛНА И CFD АНАЛИЗА ПОТИСНОГ ЛЕЖАЈА ОД ФОЛИЈЕ ПОДМАЗАНОГ ГАСОМ ЗА РАЗЛИЧИТЕ КОНФИГУРАЦИЈЕ ФОЛИЈЕ

Р.Н. Равикумар, К.Ц. Ратанрац, В. Арун Кумар, С. Суприт

Лежајеви потисне фолије који раде у хидро–динамичким условима су самодејни (аеродина–мички) лежајеви који подржавају осовине велике брзине при благим условима оптерећења са ваз–духом као мазивом и генерално се користе у гасним турбинама мале снаге. Овај рад представља екс–перименталну студију и детаљну рачунарску ана–лизу динамичких карактеристика фолије потисног лежаја (ФТБ) у погледу способности носивости у функцији брзине потисног клизача и зазора између склопа лежаја и клизача узимајући у обзир ефекат параметри лежаја као што су број фолија, облик фолија и монтажа фолија на подлогу лежаја. Параметријска студија је спроведена на новокон–цептуализованој опреми за испитивање лежајева која је способна да ротира до 45.000 обртаја у минути која је мерила аксијална оптерећења потисних лежајева ваздушне фолије (АФТБ). Рачунски модел потисних лежајева фолије за различите конфигурације са горњим фолијама симулиран је коришћењем мултифизичког софтвера за прогиб фолије и расподелу притиска на површини фолије. Нумерички резултати су упоређени са експерименталним вредностима, док су потисни лежајеви ваздушне фолије са вишеслојним фолијама названим каскадне фолије (патентиране) имали већу носивост у односу на друге конвенционалне моделе лежаја.